ARTICLE
Journal of Cellular Biochemistry 110:1439–1446 (2010)

Journal of Cellular Biochemistry

UV Light Killing Efficacy of Fluorescent Protein-Expressing Cancer Cells In Vitro and In Vivo

Hiroaki Kimura,[1,2,3] Claudia Lee,[4] Katsuhiro Hayashi,[3] Kensuke Yamauchi,[3] Norio Yamamoto,[3] Hiroyuki Tsuchiya,[3] Katsuro Tomita,[3] Michael Bouvet,[2] and Robert M. Hoffman[1,2*]

[1] *AntiCancer, Inc., 7917 Ostrow Street, San Diego, California 92111*
[2] *Department of Surgery, University of California, San Diego, 200 West Arbor Drive, San Diego, California 92103-8220*
[3] *Department of Orthopaedic Surgery, School of Medicine, Kanazawa University, Kanazawa, Ishikawa, Japan*
[4] *UVP, LLC, 2066 West 11th Street, Upland, California 91786*

ABSTRACT

We investigated the cell-killing efficacy of UV light on cancer cells expressing GFP in the nucleus and RFP in the cytoplasm (dual-color cells). After exposure to various doses of UVA, UVB, or UVC, apoptotic and viable cells were quantitated under fluorescence microscopy using dual-color 143B human osteosarcoma cells, HT-1080 human fibrosarcoma cells, Lewis lung carcinoma (LLC), and XPA-1 human pancreatic cancer cells in vitro. UV-induced cancer cell death was wave-length and dose dependent, as well as cell-line dependent. After UVA exposure, most cells were viable even when the UV dose was increased up to 200 J/m^2. With UVB irradiation, cell death was observed with irradiation at 50 J/m^2. For UVC, as little as 25 J/m^2 UVC irradiation killed approximately 70% of the 143B dual-color cells. This dose of UVB or UVA had almost no effect on the cancer cells. UV-induced cancer cell death varied among the cell lines. Cell death began about 4 h after irradiation and continued until 10 h after irradiation. UVC exposure also suppressed cancer cell growth in nude mice in a model of minimal residual cancer (MRC). No apparent side effects of UVC exposure were observed. This study opens up the possibility of UVC treatment for MRC after surgical resection. J. Cell. Biochem. 110: 1439–1446, 2010.

KEY WORDS: UVC; GFP; RFP; FLUORESCENCE IMAGING; REAL-TIME CELLULAR IMAGING; IN VITRO; IN VIVO; MINIMAL RESIDUAL CANCER

Photodynamic therapy has been shown to be effective for certain cancer types [Castano et al., 2006]. Recently, blue light was found to be photoxic for both murine and human melanoma [Sparsa et al., 2010]. UV light has been used for the phototherapy of cutaneous malignancies. Psoralen plus UVA (PUVA) and narrowband UVB were the most common phototherapy modalities used [Gilchrest et al., 1976; Hofer et al., 1999; Carter and Zug, 2009]. However, the effect of UV light on cancer cells is not well understood [Zacal and Rainbow, 2007; Benencia et al., 2008; Kim et al., 2008]. UV light has been mainly used for skin cancer, since short wavelength light does not penetrate deeply through the skin.

A major problem in surgical oncology is minimal residual cancer (MRC) after apparent tumor curative resection. For patients with no evidence of systemic metastases, metastatic relapse often occurs following resection of the primary tumor which is due to cancer cells not removed by the surgeon due to the inability to detect them. Direct identification and eradication of MRC is of particular importance and will have a significant impact on reducing the lethality of cancer [Pantel, 1999].

Our laboratory pioneered in vivo imaging with fluorescent proteins [Chishima et al., 1997; Yang et al., 2000; Hoffman, 2005]. We have also developed dual-color cancer cells, in which red fluorescent protein (RFP) is expressed in the cytoplasm and green fluorescent protein (GFP), linked to histone H2B is expressed in the nucleus. Nuclear GFP expression enables visualization of nuclear dynamics including cell cycle events and apoptosis, whereas simultaneous cytoplasmic RFP expression enables visualization of nuclear-cytoplasmic ratios as well as simultaneous cell and nuclear shape changes. Thus, total cellular dynamics can be visualized in the living dual-color cells in real time both in vitro and in vivo [Yamamoto et al., 2004; Yamauchi et al., 2005].

Additional Supporting Information may be found in the online version of this article.

*Correspondence to: Robert M. Hoffman Ph.D., AntiCancer, Inc., 7917 Ostrow St., San Diego, CA 92111.
E-mail: all@anticancer.com

Received 27 April 2010; Accepted 29 April 2010 • DOI 10.1002/jcb.22693 • © 2010 Wiley-Liss, Inc.
Published online 12 May 2010 in Wiley InterScience (www.interscience.wiley.com).

In this study, using dual-color cancer cells expressing GFP in the nucleus and RFP in the cytoplasm, we investigated the efficacy of UV light on the killing of dual-color cancer cells and determined the potential of UV light as a therapeutic modality for MRC.

MATERIALS AND METHODS

ESTABLISHMENT OF DUAL-COLOR CANCER CELL LINES

To establish dual-color cancer cells in which RFP is expressed in the cytoplasm and GFP in the nucleus, cells were transfected with retroviral DsRed-2 and histone H2B-GFP vectors as previously described [Yamamoto et al., 2004]. In brief, the *Hind*III/*Not*I fragment from pDsRed-2 (Clontech Laboratories, Inc., Palo Alto, CA), containing the full-length RFP cDNA, was inserted into the *Hind*III/*Not*I site of pLNCX2 (Clontech Laboratories, Inc.) containing the neomycin resistance gene. PT67, an NIH3T3-derived packaging cell line (Clontech Laboratories, Inc.) expressing the viral envelope, was cultured in DMEM (Irvine Scientific, Santa Ana, CA) supplemented with 10% heat-inactivated fetal bovine serum (FBS; Gemini Bio-products, Calabasas, CA). For vector production, PT67 cells, at 70% confluence, were incubated with a precipitated mixture of LipofectAMINE reagent (Life Technologies, Inc. Grand Island, NY) and saturating amounts of pLNCX2-DsRed-2 plasmid for 18 h. Fresh medium was replenished at this time. The cells were examined by fluorescence microscopy 48 h post-transfection. For selection of a clone producing high amounts of a RFP retroviral vector (PT67-DsRed-2), the cells were cultured in the presence of 200–800 μg/ml G418 (Life Technologies, Inc.) increased stepwise over 7 days [Hoffman and Yang, 2006a,b,c].

The histone H2B gene has no stop codon, thereby enabling the ligation of the H2B gene to the 5′-coding region of the GFP gene (Clontech Laboratories, Inc.) [Yamamoto et al., 2004]. The histone H2B-GFP fusion gene was then inserted at the *Hind*III/*Cal*I site of the pLHCX plasmid (Clontech Laboratories, Inc.) that has the hygromycin resistance gene. To establish a packaging cell clone producing high amounts of histone H2B-GFP retroviral vector, the pLHCX histone H2B-GFP plasmid was transfected in PT67 cells using the same methods described above for PT67-DsRed-2. The transfected cells were cultured in the presence of 200–800 μg/ml G418 (Life Technologies, Inc.) increased stepwise over 7 days.

For RFP and H2B-GFP gene transduction, 70% confluent cancer cells were used. To establish dual-color cells, clones of these cells expressing RFP in the cytoplasm were initially established. In brief, cells were incubated with a 1:1 precipitated mixture of retroviral supernatants of PT67-RFP cells and RPMI 1640 (Irvine Scientific) containing 10% FBS for 72 h. Fresh medium was replenished at this time. Cells were harvested with trypsin/EDTA 72 h post-transduction and subcultured at a ratio of 1:15 into selective medium, which contained 200 μg/ml G418. The level of G418 was increased stepwise up to 800 μg/ml [Yamamoto et al., 2004; Hoffman and Yang, 2006b].

For establishing dual-color cells, cells were then incubated with a 1:1 precipitated mixture of retroviral supernatants of PT67 H2B-GFP cells and culture medium. To select the double transformants, cells were incubated with hygromycin 72 h after transfection. The level of hygromycin was increased stepwise from 200 to 800 μg/ml (Fig. 1) [Yamamoto et al., 2004; Hoffman and Yang, 2006b].

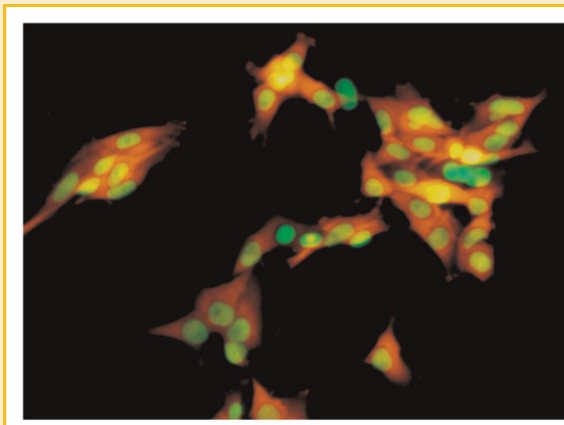

Fig. 1. Dual-color 143B human osteosarcoma cells expressing GFP in the nucleus and RFP in the cytoplasm in vitro. All cells in the population express both GFP and RFP, indicating stability of both transgenes.

CELL LINES AND CELL CULTURE

In the present study, four types of cancer cell lines were used; HT1080 human fibrosarcoma (HT1080), 143B human osteosarcoma (143B) (Fig. 1), Lewis lung carcinoma (LLC), and XPA-1 human pancreas cancer (XPA-1). These cell lines all express RFP in the cytoplasm and GFP in the nucleus. Cells were maintained in RPMI 1640 supplemented with 10% fetal bovine serum, 1% penicillin and streptomycin at 37°C in a humid atmosphere containing 5% CO_2. For in vivo studies, LLC-dual-color cells were used.

UV IRRADIATION

For UV irradiation, the cells were cultured on Lab-Tek 2 Chambered Coverglasses (Nalgen Nunc, Rochester, NY) coated with fibronectin

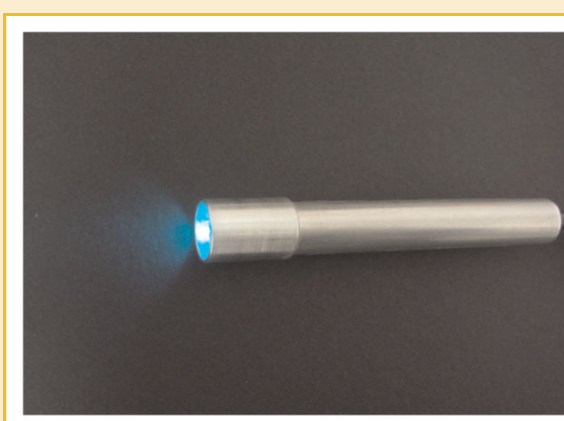

Fig. 2. Customized UVC pen light for in vivo irradiation. The pen light consisted of a quartz bulb filled with argon and mercury vapor, which emits primarily at 254 nm (UVC wavelength) encased in an aluminum cylinder. The average output power was measured at 370 $\mu W/cm^2$ at the opening of the cylinder.

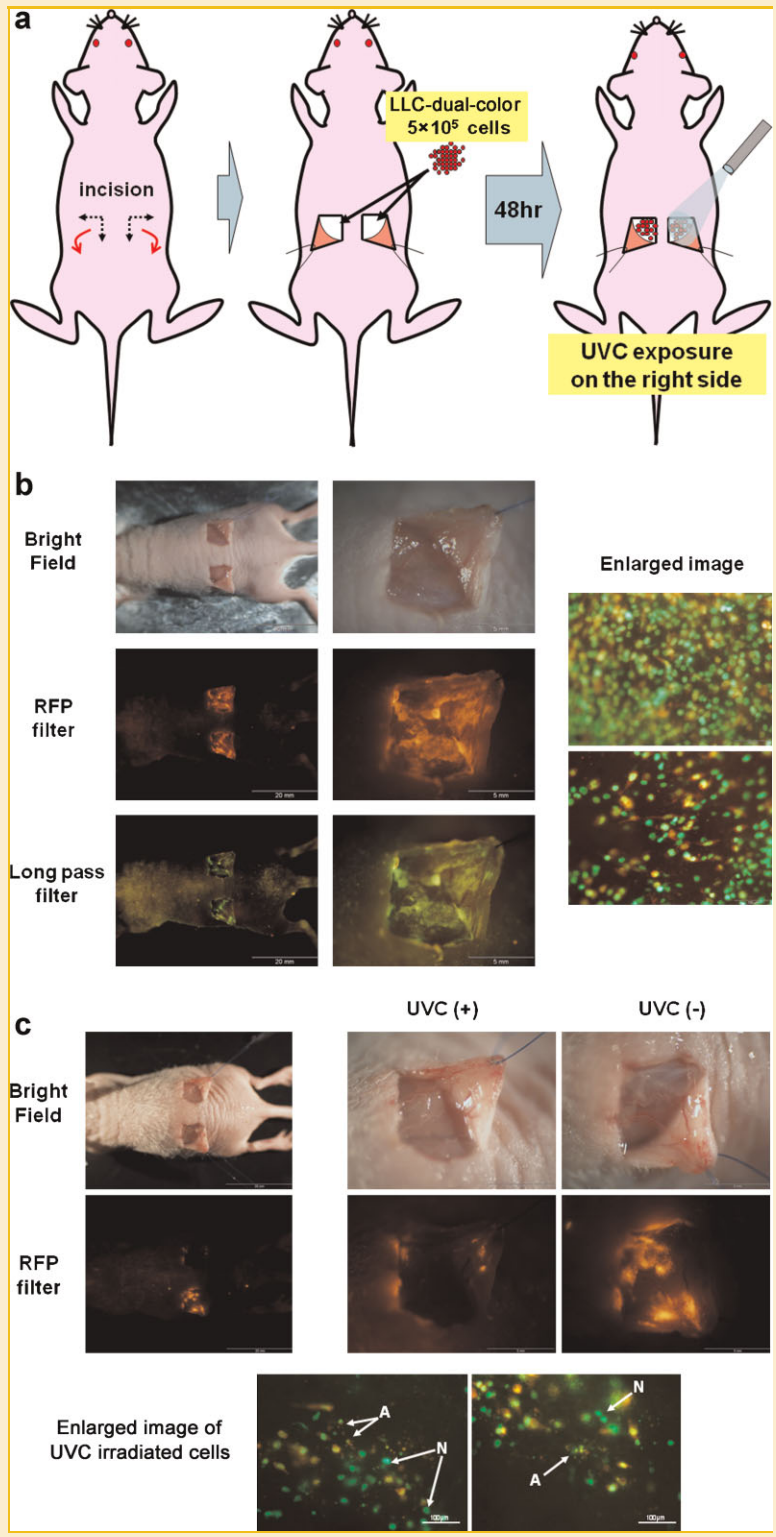

Fig. 3. UVC treatment model of minimal residual cancer in vivo. a: Diagram of minimal residual cancer (MRC) model and UVC treatment. After anesthesia, 5 mm rectangular incisions were made bilaterally on the flanks of nude mice. LLC-dual-color cells (5×10^5) in 10 μl PBS were then injected, and the incisions were closed. Forty-eight hours after cancer-cell injection, the bilateral incisions were reopened, and 100 J/m^2 UVC was irradiated only to the right-flank tumor for 180 s with the customized UVC pen light. b: Images taken 48 h after cancer cell injection. Fluorescence images show many cancer cells. c: Images 48 h after UVC irradiation showed fewer cancer cells in the irradiated flank than in the untreated flank. Enlarged images show that many irradiated cancer cells appeared apoptotic. Images were obtained with the OV100 Small Animal Imaging System (Olympus Corp.). Arrow A: apoptotic cells; Arrow N: necrotic cells.

(BD Bioscience, Bedford, MA) at 5 μg/cm^2. The cells were irradiated with UV light from the bottom of the chamber using a Benchtop 3UV transilluminator (UVP, LLC, Upland, CA), which emits UVC with an emission peak at 254 nm; UVB with an emission peak at 302 nm; and UVA with an emission peak at 365 nm. For in vivo UV irradiation, a customized UVC pen light (emission peak at 265 nm, UVP) was used (Fig. 2). The UV dose was measured with a UVX Radiometer (UVP).

UV-INDUCED CANCER CELL DEATH

To determine if UV-induced cancer cell death is dose or wavelength dependent, 143B dual-color cells were seeded into the glass chambers. After 48 h culture, the cells were irradiated with various doses UVA, UVB, or UVC (25–200 J/m^2). Twenty-four hours after irradiation, the number of apoptotic and non-apoptotic cells was determined by nuclear structure under fluorescence microscopy. Eight chambers were used for each cell line and each UV dose.

Each of the four types of cancer cell lines (143B, HT1080, LLC, and XPA-1) were irradiated with 50 J/m^2 UVC or 100 J/m^2 UVB. Twenty-four hours after irradiation, the number of apoptotic and non-apoptotic cells were counted under fluorescence microscopy. Eight chambers were used for each cell line and every UV dose.

Imaging of UV-induced cancer-cell killing was started immediately after 143B dual-color cells were irradiated with 25 J/m^2 UVC. Real-time images were captured with the OV100 Small Animal Imaging System (Olympus Corp, Tokyo, Japan) every 15 min for 12 h.

EFFICACY OF UV IRRADIATION ON MINIMAL RESIDUAL CANCER (MRC) IN VIVO

To model minimal residual cancer (MRC) after surgery, five athymic NCR nude (*nu*/*nu*) mice (Charles River Laboratories, Wilmington, MA) were first anesthetized with a ketamine mixture (10 μl ketamine HCL, 7.6 μl xylazine, 2.4 μl acepromazine maleate, and 10 μl H_2O s.c.)

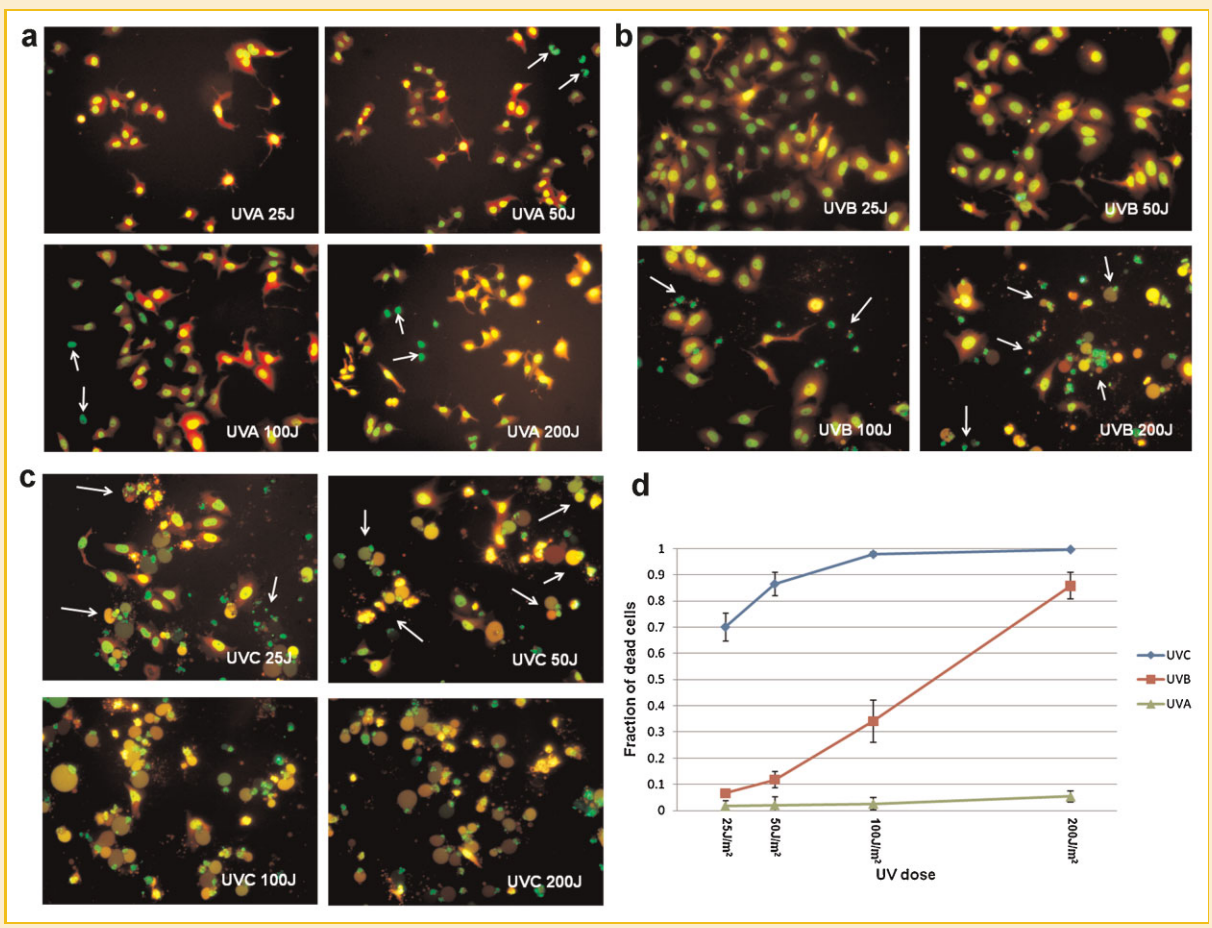

Fig. 4. Efficacy of UV irradiation on 143B cells in vitro. 143B dual-color cells were irradiated with 25, 50, 100, and 200 J/m^2 UVA, UVB, and UVC in vitro. The cells were then incubated for 24 h in a CO_2 incubator at 37°C. Under fluorescence microscopy, the number of apoptotic cells and non-apoptotic cells was counted and the morphological changes were analyzed. a: UVA irradiation of 143B dual-color cells. Most cells were viable without changing their morphology. In a few cells, the cytoplasm was shed without change in nuclear shape (arrows). b: UVB irradiation of 143B dual-color cells. Apoptotic cells began to appear among cells irradiated at 50 J/m^2 and the frequency of apoptotic cells gradually increased with higher UV exposure. Nuclear condensation and fragmentation were observed (arrows). c: UVC irradiation of 143B dual-color cells. UVC irradiation induced cancer cell death at the highest frequency. The frequency of apoptotic cells reached a plateau at 100 J/m^2. Cell shrinkage, nuclear condensation, and fragmentation were observed (arrows). d: Dose and wave-length dependency of UV-induced cell death in 143B cells. Data are the averages of eight chambers. Bars show the SD values.

via s.c. injection, Rectangular incisions (each side 5 mm) were made bilaterally on the flanks in each mouse. LLC-dual-color cells (5×10^5) in 10 μl PBS were then injected in the incised area. Incisions were closed with 6–0 sutures. Forty-eight hours after cancer cell injection, the bilateral incisions were reopened and UVC was irradiated only on the right side for 180 s with the customized UV pen light (Fig. 2). The estimated UVC exposure was 100 J/m^2. The mice were imaged once every 5 days after UVC exposure (days 5, 10, and 15), using the iBox Scientia Small Animal Imaging System (UVP) to evaluate fluorescent tumor areas (mm^2) (Fig. 3).

RESULTS

UV-INDUCED CANCER CELL DEATH WITH DIFFERENT WAVE LENGTHS AND DOSES

After exposure to various doses of UVA, UVB, or UVC, apoptotic and non-apoptotic cells were quantitated under fluorescence microscopy using the dual-color 143B cells expressing GFP in the nucleus and RFP in the cytoplasm. Cellular and nuclear morphological changes such as cell shrinkage, nuclear condensation, and fragmentation, which are features of apoptosis, were imaged.

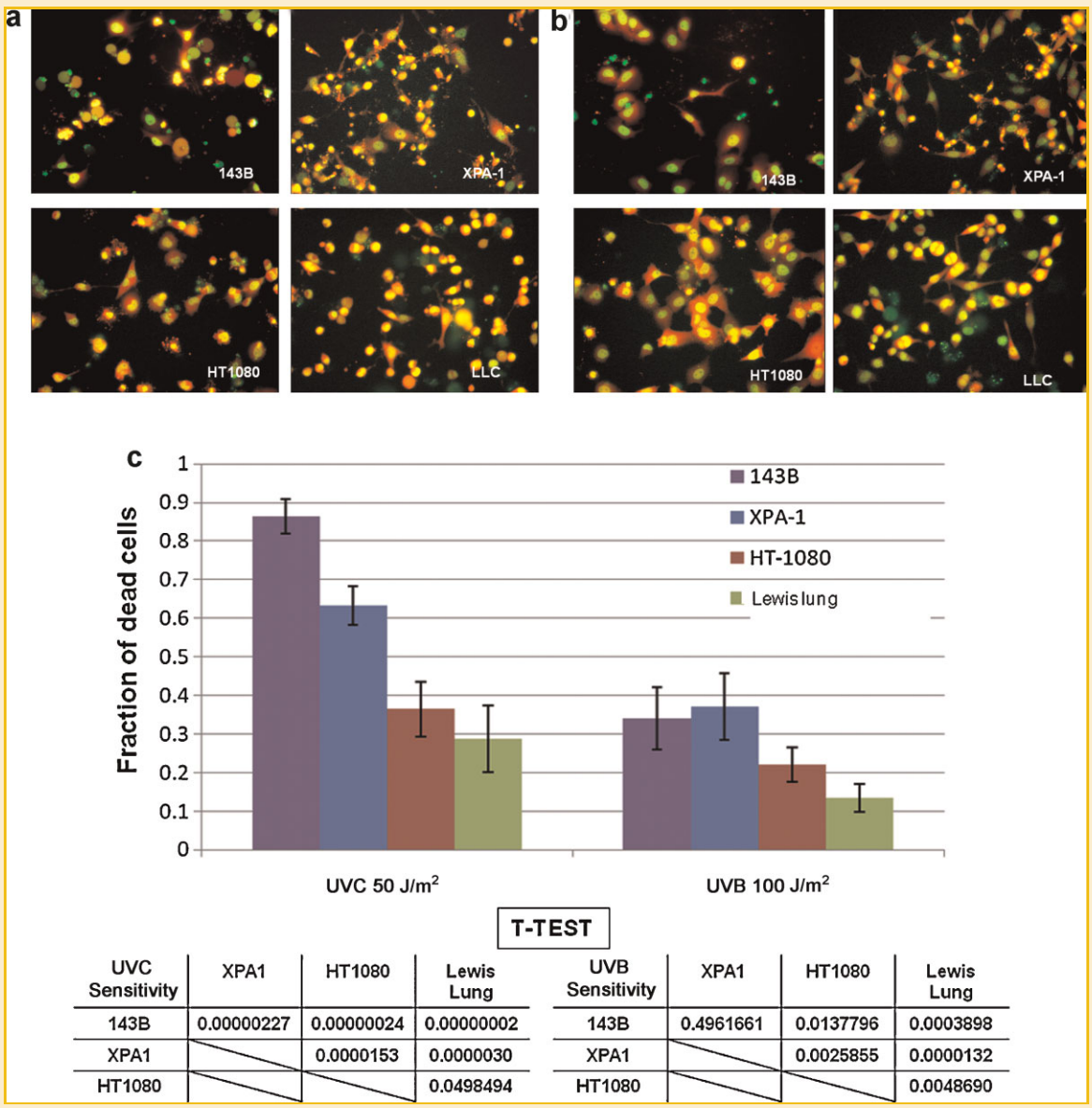

T-TEST

UVC Sensitivity	XPA1	HT1080	Lewis Lung
143B	0.00000227	0.00000024	0.00000002
XPA1		0.0000153	0.0000030
HT1080			0.0498494

UVB Sensitivity	XPA1	HT1080	Lewis Lung
143B	0.4961661	0.0137796	0.0003898
XPA1		0.0025855	0.0000132
HT1080			0.0048690

Fig. 5. Efficacy of 50 J/m^2 UVC and 100 J/m^2 UVB irradiation on different cancer cell lines in vitro. UVC (50 J/m^2) or UVB (100 J/m^2) were irradiated on four different types of cancer cell lines (143B, HT1080, XPA-1, and LLC). The number of apoptotic cells was counted under fluorescence microscopy after 24 h subsequent culture. a: 50 J/m^2 UVC. 143B cells were the most sensitive to UVC light. The morphology of apoptotic cells varied slightly among the cell lines. b: 100 J/m^2 UVB. The cell lines had the same relative sensitivity to UVB as UVC. c: Data are the averages of eight chambers. Bars show the SD values. Statistical differences were analyzed using the Student's *t*-test. This figure indicates that the sensitivity to UV irradiation varied among cell lines.

Twenty-four hours after UVA exposure, most cells were viable without change in morphology, even when the UVA dose was increased up to 200 J/m^2 (Fig. 4a).

After UVB irradiation, apoptotic cells began to appear at 50 J/m^2. With 200 J/m^2 UVB, approximately 85% of the irradiated cells became apoptotic as determined by nuclear condensation and fragmentation. In a few cells, the cytoplasm was rounded without change in nuclear shape (Fig. 4b).

UVC irradiation induced cancer cells apoptosis at the highest frequency. As little as 25 J/m^2 UVC irradiation killed approximately 70% of 143B dual-color cells. The frequency of cell killing plateaued at 100 J/m^2. The morphological features of UVC irradiated cells were similar to those irradiated by UVB, in which cell shrinkage, nuclear condensation, and fragmentation occurred (Fig. 4c).

These results indicated that UV-induced cancer cell death was wave-length and dose dependent (Fig. 4d).

UV-INDUCED CANCER CELL DEATH IN DIFFERENT CELL LINES

143B, HT1080, LLC, and XPA-1 dual-color cells were irradiated with 50 J/m^2 UVC or 100 J/m^2 UVB, based on the data described above. Twenty-five hours after 50 J/m^2 UVC irradiation, over 80% of the 143B cells became apoptotic, whereas less than 30% of the LLC cells became apoptotic (Fig. 5a). UVB irradiation was also more effective on 143B cells than on LLC cells (Fig. 5). The other cell lines were intermediately sensitive to UVC and UVB (Fig. 5). This result showed the sensitivity to UV irradiation was cell-line dependent.

REAL-TIME IMAGING OF CANCER CELL APOPTOSIS AND NECROSIS INDUCED BY UV LIGHT

During real-time imaging, changes in cell morphology occurred due to UV irradiation, such as ruffled edges, condensed chromatin and nuclear fragmentation, cell shrinkage, formation of apoptotic bodies, and shedding of cytoplasm. These events occurred between 4 and 10 h after UVC irradiation. Most cells appeared to undergo apoptosis. In a few cells, sudden shedding of cytoplasm was observed without change in nuclear shape. Cytoplasmic shedding could be observed between 3 h and 7 h after irradiation (Fig. 6 and Supplementary Movie 1).

UVC LIGHT TREATMENT OF MINIMAL RESIDUAL CANCER

UVC irradiation suppressed tumor growth in all five treated mice (Fig. 7a). The average fluorescent area of LLC-dual-color tumors on the untreated flank was significantly larger than on the UVC irradiation side at days 5, 10, and 15 (Fig. 7b). In one mouse, UVC irradiation completely inhibited tumor formation. No apparent side effects of UVC exposure were observed.

DISCUSSION

During surgical resection of tumors, viable tumor cells are commonly shed into the surgical field [Umpleby et al., 1984; Allardyce et al., 1996; Jayne et al., 2007]. Tumor tissue often goes undetected by the surgeon as well [Frost and Levin, 1992]. Furthermore, tumors are often removed with inadequate or poor margin during surgery. Residual cancer cells may cause tumor recurrence [Pratt et al., 1999; Nordlinger et al., 2005; Strohlein and Heiss, 2007]. Despite the introduction of multimodal treatments for MRC, tumor recurrence is extremely common. Elimination of MRC after cancer surgery with an effective modality would be a major advance.

Our results indicated UV light could induce apoptosis in cancer cells. The data in the present report indicates that shorter wavelength UV light was more effective to kill cancer cells in vitro. Therefore, we utilized UVC for the treatment of MRC in mice. Although UVC light does not deeply penetrate tissue, we assumed that it could be

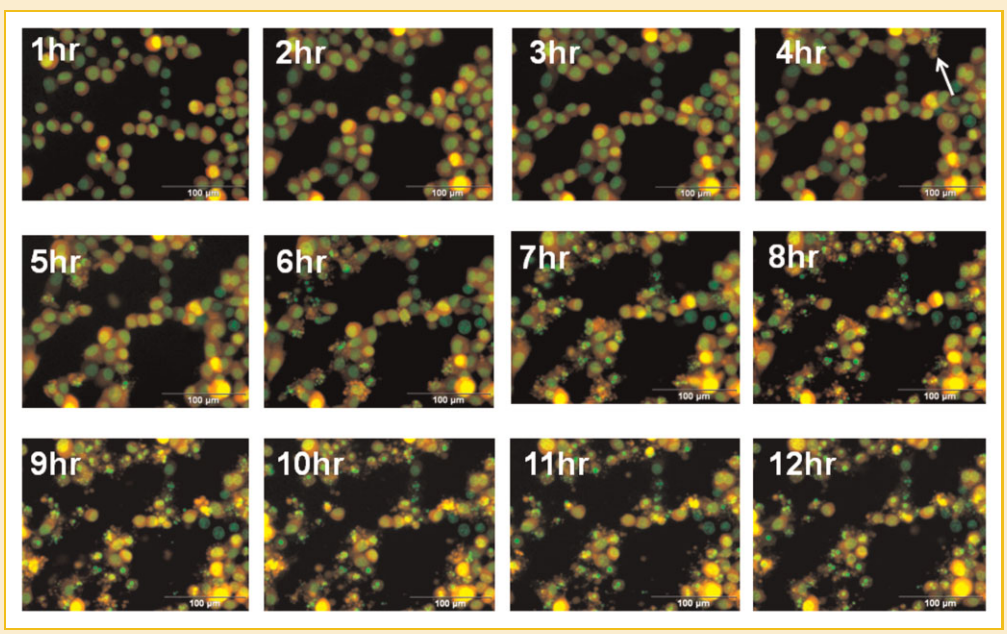

Fig. 6. Real-time imaging of 143B cancer cell death induced by UVC in vitro. 143B dual-color cells were irradiated with 25 J/m^2 UVC. Images were captured with the OV100 Small Animal Imaging System every 15 min for 12 h. Real-time imaging showed that cell death began approximately 4 h after irradiation and continued until 10 h after irradiation. Most cells died via apoptosis, which had a sudden onset. Arrow shows the first apoptotic cell that died 4 h after eradication. See also Supplemental Movie 1.

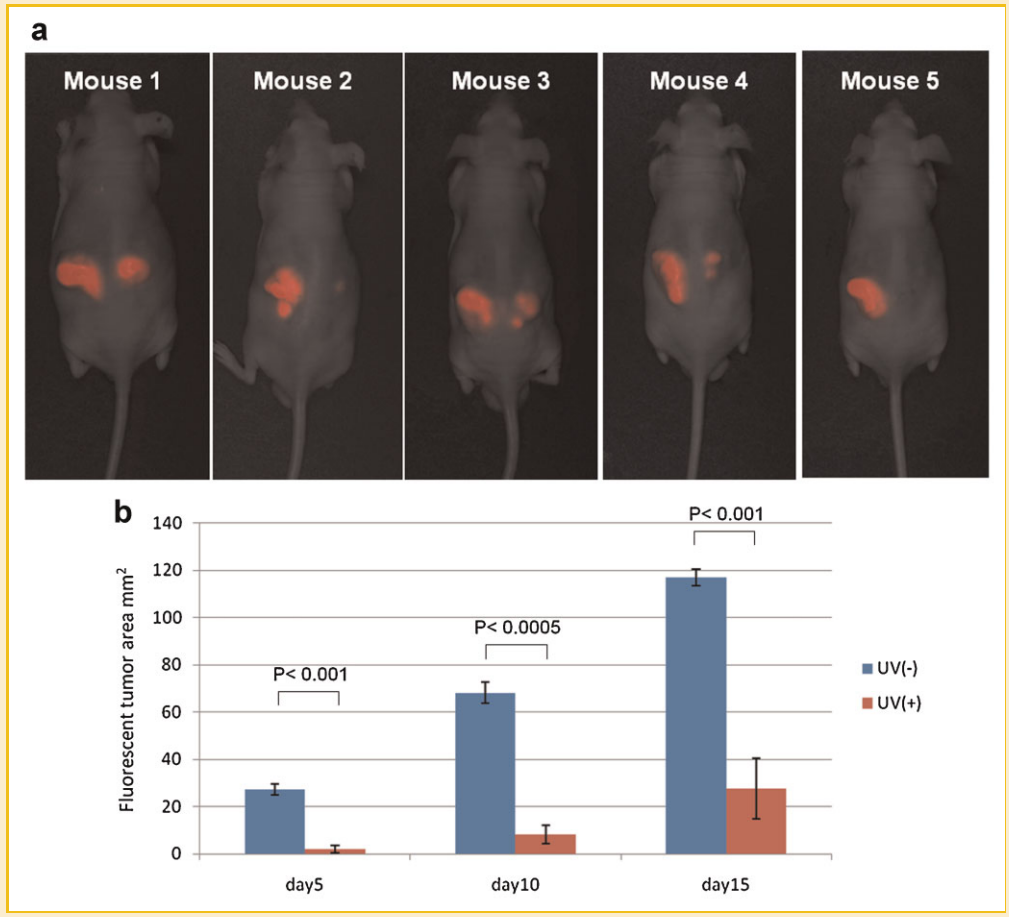

Fig. 7. Efficacy of UVC irradiation on the minimal residual cancer model in vivo. UVC was irradiated on the right-flank tumor. The left-flank tumor was untreated. The mice were imaged once every 5 days, using the iBox Scientia Small Animal Imaging System (UVP) with an RFP filter. a: Merged images of bright field and RFP fluorescence at day 15. In all mice, the right-side tumors, which were irradiated with UVC, were smaller than the untreated left-side tumors. In mouse 5, UVC exposure completely inhibited tumor formation. b: Fluorescent area (mm^2) of residual tumors at days 5, 10, and 15. Blue bars are the untreated left-flank tumors and red bars are the treated right-flank tumors. The experimental data were expressed as the mean ± SD of 5 mice. The statistical difference between UV-treated and untreated tumor sizes was analyzed using the Student's *t*-test. The average tumor size of the UV-treated group was significantly smaller than the untreated group.

effective in preventing tumor formation from MRC and minimize the side effects of UV treatment on normal tissue. The present study showed that UVC irradiation of MRC inhibited subsequent tumor formation and without any obvious side effects.

This study opens up the possibility of UVC treatment for MRC after surgical resection. This possibility is even more exciting due to our recent development of labeling tumors in situ with GFP using a tumor-specific telomerase-dependent adenovirus containing the GFP gene [Kishimoto et al., 2006, 2009a,b]. UV light treatment could be then applied to MRC after fluorescence-guided surgery of cancer labeled with adenoviral GFP. GFP expression in the MRC cells would aid their detection and guide UV light treatment. This approach has promising clinical potential.

REFERENCES

Allardyce R, Morreau P, Bagshaw P. 1996. Tumor cell distribution following laparoscopic colectomy in a porcine model. Dis Colon Rectum 39(10 Suppl): S47–S52.

Benencia F, Courrèges MC, Coukos G. 2008. Whole tumor antigen vaccination using dendritic cells: Comparison of RNA electroporation and pulsing with UV-irradiated tumor cells. J Transl Med 6:21.

Carter J, Zug KA. 2009. Phototherapy for cutaneous T-cell lymphoma: Online survey and literature review. J Am Acad Dermatol 60:39–50.

Castano AP, Liu Q, Hamblin MR. 2006. A green fluorescent protein-expressing murine tumour but not its wild-type counterpart is cured by photodynamic therapy. Br J Cancer 94:391–397.

Chishima T, Miyagi Y, Wang X, Yamaoka H, Shimada H, Moossa AR, Hoffman RM. 1997. Cancer invasion and micrometastasis visualized in live tissue by green fluorescent protein expression. Cancer Res 57:2042–2047.

Frost P, Levin B. 1992. Clinical implications of metastatic process. Lancet 339:1458–1461.

Gilchrest BA, Parrish JA, Tanenbaum L, Haynes HA, Fitzpatrick TB. 1976. Oral methoxsalen photochemotherapy of mycosis fungoides. Cancer 38:683–689.

Hofer A, Cerroni L, Kerl H, Wolf P. 1999. Narrowband (311-nm) UV-B therapy for small plaque parapsoriasis and early-stage mycosis fungoides. Arch Dermatol 135:1377–1380.

Hoffman RM. 2005. The multiple uses of fluorescent proteins to visualize cancer in vivo. Nat Rev Cancer 5:796–806.

Hoffman RM, Yang M. 2006a. Subcellular imaging in the live mouse. Nat Protoc 1:775–782.

Hoffman RM, Yang M. 2006b. Color-coded fluorescence imaging of tumor-host interactions. Nat Protoc 1:928–935.

Hoffman RM, Yang M. 2006c. Whole-body imaging with fluorescent proteins. Nat Protoc 1:1429–1438.

Jayne DG, Guillou PJ, Thorpe H, Quirke P, Copeland J, Smith AM, Heath RM, Brown JM. 2007. Randomized trial of laparoscopic-assisted resection of colorectal carcinoma: 3-year results of the UK MRC CLASICC Trial Group. J Clin Oncol 25:3061–3068.

Kim SC, Park S-S, Lee YJ. 2008. Effect of UV irradiation on colorectal cancer cells with acquired TRAIL resistance. J Cell Biochem 104:1172–1180.

Kishimoto H, Kojima T, Watanabe Y, Kagawa S, Fujiwara T, Uno F, Teraishi F, Kyo S, Mizuguchi H, Hashimoto Y, Urata Y, Tanaka N, Fujiwara T. 2006. In vivo imaging of lymph node metastasis with telomerase-specific replication-selective adenovirus. Nat Med 12(10): 1213–1219.

Kishimoto H, Zhao M, Hayashi K, Urata Y, Tanaka N, Fujiwara T, Penman S, Hoffman RM. 2009a. In vivo internal tumor illumination by telomerase-dependent adenoviral GFP for precise surgical navigation. Proc Natl Acad Sci USA 106:14514–14517.

Kishimoto H, Urata Y, Tanaka N, Fujiwara T, Hoffman RM. 2009b. Selective metastatic tumor labeling with green fluorescent protein and killing by systemic administration of telomerase-dependent adenoviruses. Mol Cancer Ther 8:3001–3008.

Nordlinger B, Rougier P, Arnaud JP, Debois M, Wils J, Ollier JC, Grobost O, Lasser P, Wals J, Lacourt J, Seitz JF, Guimares dos Santos J, Bleiberg H, Mackiewickz R, Conroy T, Bouché O, Morin T, Baila L, van Cutsem E, Bedenne L. 2005. Adjuvant regional chemotherapy and systemic chemotherapy versus systemic chemotherapy alone in patients with stage II–III colorectal cancer: A multicentre randomised controlled phase III trial. Lancet Oncol 6:459–468.

Pantel K. 1999. Minimal residual disease. Introductory overview. Cancer Metastasis Rev 18:1–2.

Pratt CB, Pappo AS, Gieser P, Jenkins JJ, Salzbergdagger A, Neff J, Rao B, Green D, Thomas P, Marcus R, Parham D, Maurer H. 1999. Role of adjuvant chemotherapy in the treatment of surgically resected pediatric nonrhabdomyosarcomatous soft tissue sarcomas: A Pediatric Oncology Group study. J Clin Oncol 17:1219.

Sparsa A, Faucher K, Sol V, Durox H, Boulinguez S, Doffoel-Hantz V, Calliste CA, Cook-Moreau J, Krausz P, Sturtz FG, Bedane C, Jauberteau-Marchan MO, Ratinaud MH, Bonnetblanc JM. 2010. Blue light is phototoxic for B16F10 murine melanoma and bovine endothelial cell lines by direct cytocidal effect. Anticancer Res 30:143–1147.

Strohlein M, Heiss M. 2007. Immunotherapy of peritoneal carcinomatosis. In: Ceelen W, editor. Peritoneal carcinomatosis: A multidisciplinary approach. New York: Springer. pp 483–491.

Umpleby HC, Fermor B, Symes MO, Williamson RC. 1984. Viability of exfoliated colorectal carcinoma cells. Br J Surg 71:659–663.

Yamamoto N, Jiang P, Yang M, Xu M, Yamauchi K, Tsuchiya H, Tomita K, Wahl GM, Moossa AR, Hoffman RM. 2004. Cellular dynamics visualized in live cells in vitro and in vivo by differential dual-color nuclear-cytoplasmic fluorescent-protein expression. Cancer Res 64:4251–4256.

Yamauchi K, Yang M, Jiang P, Yamamoto N, Xu M, Amoh Y, Tsuji K, Bouvet M, Tsuchiya H, Tomita K, Moossa AR, Hoffman RM. 2005. Real-time in vivo dual-color imaging of intracapillary cancer cell and nucleus deformation and migration. Cancer Res 65:4246–4252.

Yang M, Baranov E, Jiang P, Sun F-X, Li X-M, Li L, Hasegawa S, Bouvet M, Al-Tuwaijri M, Chishima T, Shimada H, Moossa AR, Penman S, Hoffman RM. 2000. Whole-body optical imaging of green fluorescent protein-expressing tumors and metastases. Proc Natl Acad Sci USA 97:1206–1211.

Zacal N, Rainbow AJ. 2007. Photodynamic therapy resistant human colon carcinoma HT29 cells show cross-resistance to UVA but not UVC Light. Photochem Photobiol 83:730–737.